Theoretical Characterization of End-On and Side-On Peroxide Coordination in Ligated Cu₂O₂ Models

Christopher J. Cramer,*,† Armagan Kinal,‡ Marta Włoch,‡ Piotr Piecuch,‡,§ and Laura Gagliardi⊥

Department of Chemistry and Supercomputer Institute, University of Minnesota, 207 Pleasant Street SE, Minneapolis, Minnesota 55455, Department of Chemistry and Department of Physics and Astronomy, Michigan State University, East Lansing, Michigan 48824, and Department of Physical Chemistry, Sciences II, University of Geneva, 30 Quai Ernest Ansermet, CH-1211 Geneva 4, Switzerland

The relative energetics of μ-η^1:η^1 (trans end-on) and μ-η^2:η^2 (side-on) peroxo isomers of Cu₂O₂ fragments supported by 0, 2, 4, and 6 ammonia ligands have been computed with various density functional, coupled-cluster, and multiconfigurational protocols. There is substantial disagreement between the different levels for most cases, although completely renormalized coupled-cluster methods appear to offer the most reliable predictions. The significant biradical character of the end-on peroxo isomer proves problematic for the density functionals, while the demands on active space size and the need to account for interactions between different states in second-order perturbation theory prove challenging for the multireference treatments. In the latter case, it proved impossible to achieve any convincing convergence.

Introduction

Interest in molecules containing Cu₂O₂ fragments has been motivated by the characterization of a number of metalloenzymes containing one, two, or more copper atoms that activate molecular oxygen so as to oxidize organic substrates.[1–8] Tyrosinase[1,5,6,9] is one example of an enzyme whose active site incorporates a Cu₂O₂ core, and substantial effort has also been devoted to the characterization of smaller inorganic models characterized by the same core.[2,10–18]

There are several motifs for the binding of molecular O₂ to two supported copper(I) atoms (Figure 1).[12,19] Best characterized experimentally (because they have been observed for many different supporting ligand sets) are the side-on μ-η^2:η^2 peroxo and the bis(μ-oxo). The trans end-on μ-η^1:η^1 peroxo motif was first described by Jacobson et al.[20] This binding mode is preferred when the copper atoms are supported by tripodal tetradentate ligands,[21–25] although when such ligands become too sterically demanding for trigonal bipyramidal coordination of copper a preference for the bis(μ-oxo) motif with concomitant loss of two ligand–copper interactions has been documented.[26] Only rare examples of the other three cases shown in Figure 1 have been documented or proposed. In certain cases, it has been demonstrated that more than one binding mode can be accessed. For instance, and of particular relevance to the present paper, Jung et al.[27] have demonstrated that the binding of oxygen to a dicopper complex supported by a bridging *N,N,N′,N′*-bis{2-(2-pyridyl)ethyl}-1,4-butanediamine ligand shows a kinetic preference for end-on peroxo but a thermodynamic preference for side-on peroxo.

In prior work, we examined the ability of different theoretical models to predict accurately the relative energetics of the side-
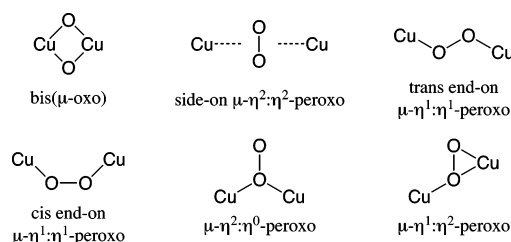

Figure 1. Binding motifs for Cu₂O₂.

on peroxo and bis(μ-oxo) forms.[28] These two structures have been demonstrated to have similar energetics with selected ligand sets[11,13,21,26,29–34] and on that basis this equilibrium has been suggested to have possible relevance for the mechanism of oxytyrosinase. We found that this equilibrium was surprisingly difficult to model, mostly because of how difficult it proved to maintain a balanced description of rapidly varying dynamical and nondynamical electron correlation effects along isomerization coordinates linking the two structures, each of which has associated biradical character that depends on the number of supporting ligands. We found that the completely renormalized (CR) coupled-cluster (CC) levels of theory including triple excitations, particularly the recently formulated, rigorously size extensive CR-CCSD(T)$_L$ model (referred to here and elsewhere in this work as CR-CC(2,3),D) and their extensions to quadruple excitations, agreed well with pure density functional levels of theory—which were particularly efficient as theoretical models—and that predictions from these models were in qualitative agreement with experimental results for Cu₂O₂ cores supported by ligand sets too large to be practically treated at the coupled-cluster level. Standard coupled-cluster methods (i.e., not renormalized) such as CCSD(T) were less accurate and, unlike CR-CC, exhibited poor convergence in predicted relative energies when corrected for the effects of higher-than-triple excitations and other high-order correlations neglected in CCSD(T). Hybrid density functionals underesti-
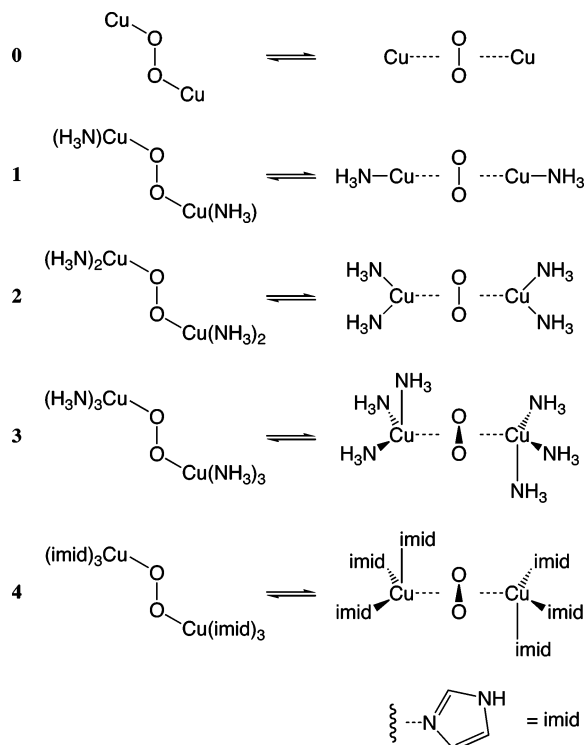
---
† University of Minnesota.
‡ Department of Chemistry, Michigan State University.
§ Department of Physics and Astronomy, Michigan State University.
⊥ University of Geneva.

SCHEME 1

mated the stability of the bis(μ-oxo) form by a large amount (with the magnitude of the error being directly proportional to the percentage Hartree−Fock exchange in the functional), and single-root multireference second-order perturbation theory (CASPT2) *overestimated* the stability of these same isomers. With the latter model, it proved difficult to demonstrate convergence in relative energies within practical limitations on active space size.

In this work, we extend our consideration to the trans end-on peroxo isomer. In particular, we compare several different density functional (DFT) models, single- and multistate multireference second-order perturbation theory (CASPT2 and MS-CASPT2), and standard and completely renormalized (CR) coupled-cluster (CC) methods with respect to their abilities to predict accurate energetics for the conversion of the μ-η^1:η^1 Cu$_2$O$_2^{2+}$ core to its μ-η^2:η^2 isomer. We consider five ligand sets (Scheme 1), namely, no ligands at all (**0**), one (**1**), two (**2**), and three (**3**) ammonia ligands per copper atom, and three imidazole ligands (**4**) per copper atom.

Theoretical Methods

Basis Sets. Four different basis sets including a copper relativistic core pseudopotential (the Stuttgart 10-electron pseudopotential and associated basis functions[35]) were used in this work, which we name BS1, BS2, BS3, and BS4. BS1 and BS2 used the atomic natural orbital (ANO) basis set of Pierloot et al.[36] for light atoms. A [10s6p3d | 4s3p2d] contraction was used in BS1 for N and O, while for H we used an [8s4p | 2s1p] contraction. In BS2, the same primitive functions were contracted as 4s2p1d and 2s, respectively. BS3 was used only for geometry optimizations of **0**−**3** and employed the Pople basis set 6-31G(d) for H, N, and O.[37] BS4 was used only for **4** and consisted of the Pople basis sets[37] STO-3G and 6-311G(d) for H and O, respectively, and the MIDI! basis set[38] for C and N.

As part of a study on basis set effects, two additional basis sets were employed for certain calculations. These basis sets

were modifications of BS1 in which an all-electron basis set[39] was used for copper in place of the Stuttgart pseudopotential. In BS1d the copper contraction was [21s15p10d6f | 5s4p2d1f], while in BS1t the same primitives were contracted as 6s5p3d2f (a [4g | 1g] contraction was also included in CAS and CASPT2 calculations).

Density Functionals. We assayed three different pure functionals. The BLYP functional combines the generalized-gradient approximation (GGA) exchange functional of Becke[40] with the GGA correlation functional of Lee, Yang, and Parr.[41] The *m*PWPW91 functional combines the GGA exchange[42] and correlation[43] functionals of Perdew and Wang as modified by Adamo and Barone.[44] The TPSS functional is a meta-GGA functional.[45]

We also considered hybrid HF-DFT functionals.[46] The B3LYP,[47] *m*PW1PW91,[44] MPW1K,[48] and TPSSh[49] functionals incorporate 20%, 25%, 48.2%, and 10% HF exchange, respectively, into their corresponding functionals.

For singlet state calculations, unstable restricted (R) self-consistent field (SCF) solutions were reoptimized at the unrestricted (U) SCF level.[50] All restricted solutions were checked for instability. Singlet energies from unrestricted calculations were computed in two ways. First, the raw broken-spin-symmetry (BS) SCF energy was used without modification. Second, the sum method[51] was employed to eliminate spin contamination from the triplet state in the SCF solution. In this approach the singlet energy is computed as[52−54]

$$E_{singlet} = \frac{2E_{\langle S_z \rangle = 0} - \langle S^2 \rangle E_{\langle S_z \rangle = 1}}{2 - \langle S^2 \rangle} \tag{1}$$

where the triplet energy is computed for the single-determinantal high-spin configuration $S_z = 1$ (at the BS geometry) and $\langle S^2 \rangle$ is the expectation value of the total-spin operator applied to the Kohn−Sham (KS) determinant for the unrestricted $S_z = 0$ calculation. Gräfenstein and Cremer[55] have shown that values of $\langle S^2 \rangle$ computed at the DFT level have diagnostic value in assessing spin contamination, so the sumBS approach is more physically realistic than using the raw BS energy.

Single-Reference Post-SCF Levels. We performed a variety of standard single-reference CC calculations[56,57] using the CC method with singles and doubles (CCSD),[58−60] the CC method with singles, doubles, and noniterative triples (CCSD(T)),[61] and, to explore the role of higher-order correlations, the CC method with singles, doubles, and noniterative triples and quadruples (CCSD(TQ)), using variant "b" of the factorized CCSD(TQ) approximation.[62]

To improve on the CC model, we performed calculations using the recently developed[62−67] completely renormalized CCSD(T) (CR-CCSD(T)) and CCSD(TQ) (CR-CCSD(TQ)) methods which can accurately and effectively deal with reactive potential energy surfaces involving bond stretching,[63−73] biradicals,[28,74−76] and other cases of electronic near-degeneracies within a single-reference description employing an RHF reference. We used variant "b" of the CR-CCSD(TQ) approach,[62] which enables us to determine if the CR-CCSD(T) results are reasonably well converged with respect to higher-order correlation effects. While the CR-CCSD(T) and CR-CCSD(TQ) approaches provide a robust description of biradical systems, they slightly violate the rigorous size extensivity of CC theory (at the level of 0.5−1.0% of the changes in the correlation energy along a reaction pathway). Also, certain types of high-order dynamical correlations which are represented, for example, as disconnected products of singly, doubly, and triply excited

Peroxide Coordination in Ligated Cu$_2$O$_2$ Models

J. Phys. Chem. A, Vol. 110, No. 40, 2006 **11559**

clusters and which may play a role in the systems examined in this study, are neglected at the CR-CCSD(T) level (as they are also in CCSD(T)). To address the issues of convergence with respect to higher-order correlations neglected in CR-CCSD(T) and size extensivity, we also performed calculations using the recently proposed rigorously size extensive CR-CC(2,3) approach, which is based on a new, biorthogonal formulation of the method of moments of CC equations (a formalism used to design all CR-CC methods[63−65,67]) employing the left eigenstates of the similarity-transformed Hamiltonian of CC theory.[77−79] Two sets of the CR-CC(2,3) data are reported. The best CR-CC(2,3) results are obtained using the most complete CR-CC-(2,3),D approximation, which exploits the diagonal part of the triples−triples block of the similarity-transformed Hamiltonian of CCSD in the design of the relevant completely renormalized triples correction to CCSD energy. The CR-CC(2,3),D approach (referred to as CR-CCSD(T)$_L$ in the prior work[28] and the original ref 78) represents the most accurate noniterative triples CC method formulated to date (better, in particular, than CCSD(T) and CR-CCSD(T)). We also present the CR-CC(2,3),A data, which correspond to the more approximate treatment of the triples correction within the CR-CC(2,3) formalism. In the CR-CC(2,3),A approximation, one uses plain orbital energy differences that define triple excitations instead of the diagonal part of the triples−triples block of the similarity-transformed Hamiltonian of CCSD in the design of the corresponding triples energy correction. The CR-CC(2,3),A approach is equivalent to the CCSD(2)$_T$ method introduced in ref 80, and its performance is usually similar to that of the older CR-CCSD(T) approach, but neither CR-CC(2,3),A nor CR-CCSD(T) are as good as CR-CC(2,3),D. The reader is referred to refs 77 and 81 for further details regarding the A−D variants of CR-CC(2,3). In addition to being size extensive and more accurate than CR-CCSD(T) and CR-CC(2,3),A=CCSD(2)$_T$, the most complete CR-CC-(2,3),D approximation offers several other useful features. It is, for example, at least as accurate as CCSD(T) for nondegenerate closed-shell states, while being as effective in describing bond breaking and biradicals as the highly accurate, but prohibitively expensive, full CC theory with singles, doubles, and triples (full CCSDT). Since the corresponding quadruples approximation, termed CR-CC(2,4), has not been implemented yet, we estimate the effect of quadruples on the CR-CC(2,3),D results by adding the Q correction, defined as CR-CCSD(TQ)−CR-CCSD(T), to CR-CC(2,3),D energies. The resulting approach, designated here and elsewhere in this article as CR-CC(2,3)+Q (called in the prior work[28] CR-CCSD(TQ)$_L$), has been shown to be very accurate in the calculations involving reactive potential energy surfaces involving single- and at least some types of double-bond breaking, providing the results that can compete with the best multireference configuration interaction calculations,[81] which cannot be afforded for systems studied in this work. For biradicals, CR-CC(2,3)+Q and CR-CC(2,3),D results are very similar and the prior[28] and present studies confirm this.

In all single-reference correlated calculations, we used the RHF determinant that we identified as the lowest-energy symmetry-adapted RHF solution as a reference. The RHF, second-order many-body perturbation theory (MBPT(2) or MP2), CCSD(T), CR-CCSD(T), and CR-CC(2,3) calculations were performed for all systems up to **3**. The smaller BS2 basis set was used for CR-CC(2,3) calculations on **3** (all other CC and CR-CC calculations were carried out with BS1). Because of resource demands, CR-CCSD(TQ)/BS1 and the corresponding CR-CC(2,3)+Q/BS1 calculations were carried out for **0** and

1 only. We explicitly correlated the 4s and 3d electrons of the Cu atoms, the 2s and 2p electrons of the N and O atoms, and the 1s electrons of the H atoms.

Multireference SCF and Post-SCF Levels. The complete active space (CAS) SCF method[82] was used to generate molecular orbitals (MOs) and reference functions for subsequent multiconfigurational second-order perturbation calculations of the dynamic correlation energy (CASPT2).[83] In addition to single-root CAS calculations, several electronic states (up to five) were included in state-averaged calculations and subsequently allowed to interact via the multistate CASPT2 formalism (MS-CASPT2). MS-CASPT2 takes into account the coupling of multiple electronic states at second order via an effective Hamiltonian, the diagonalization of which provides improved state energies.[84] In CASPT2 and MS-CASPT2 calculations, N and O 1s orbitals and Cu orbitals up to 3s were kept frozen. In addition, all such calculations employed a real level shift[85] of 0.1 au in combination with a technique[86] that shifts active space orbital energies in order to simulate ionization energies for orbitals from which excitations are taking place and electron affinities for orbitals into which excitations are taking place. In the cases examined here, however, intruder states did not appear to pose any significant problems, at least for the low-lying roots in each set of calculations. When BS1d and BS1t were used as basis sets, relativistic effects were accounted for using a Douglas−Kroll−Hess Hamiltonian.[87,88]

The performance of the CASSCF/CASPT2 model, which has been widely used for the quantitative modeling of various aspects of transition-metal chemistry,[89−91] depends critically on the choice of the orbital active space for the CAS reference. In our earlier work focusing on the μ-η^2:η^2 peroxo/bis(μ-oxo) equilibrium,[28] we found that no accessible active space gave a satisfactory description of all structures along the isomerization coordinate. The situation was not found to be improved in the present study. To describe the μ-η^2:η^2 peroxo/μ-η^1:η^1 peroxo equilibrium, it seems that the removal of almost any small number of valence orbitals from the active space leads to significant instability. The full valence space includes the 2s and 2p orbitals of the two oxygen atoms and the 3d orbitals of the two copper atoms (and moreover Cu 4d orbitals may also be needed in order to describe the double-shell effect), and this size active space is certainly not practical. We have tried to reduce the active space in various ways. For example, we tried to construct an active space formed by molecular orbitals which were linear combinations of the 2p O and the 3d$_{xy}$ and 4d$_{xy}$ Cu orbitals (all heavy atoms in **0**, **1**, and **2** being placed in the *xy* plane). This gives an active space of 12 electrons in 10 orbitals, but predicted energetics are *very* different from those computed at the CR-CC levels (and also substantially different from DFT). We have extended this (12,10) active space in various ways, up to at most a (16,14) active space, without achieving any systematic agreement with the CR-CC models. In general, no convergence in relative energies was achieved with increasing active space size, suggesting that none were adequate.

State-averaged CASSCF calculations using several roots and, in some cases, the corresponding MS-CASPT2 calculations, gave results very different from single-root results. Strong interactions between the ground-state root and higher roots were observed with certain active spaces, but again no systematic pattern emerged. With each added root the wave functions and relative energies changed dramatically, indicating them likely to be artifacts of too small an active space.

Attempts were made to include additional correlations by permitting the wave functions to have lower symmetry than that

of the overall system, to include the imposition of no symmetry at all. While this led to apparent convergence of wave functions and relative energies with respect to active space size, predicted energetics became very different from those predicted at the best CR-CC levels. In the absence of a second-order perturbation theory treatment that is compatible with a restricted active space (RAS), as opposed to a CAS, it appears that the multireference models used in this work cannot be used for the reliable study of the Cu_2O_2 motif, and we report results here primarily for technical experts who may find them useful in future methods development. Of course, it is possible that an arbitrarily selected active space in any one of our systems may provide a quantitatively accurate description of the isomerization energetics. However, any such result could only be regarded as fortuitous, insofar as it proved impossible to demonstrate convergence in relative energies with respect to active space size in any of the cases examined here.

Geometries. All geometries were fully optimized at the UB3LYP/BS3 level. The geometries of systems **0** and **1** belonged to the C_{2h} point group; those for **2** and **3** belonged to the C_i point group. Intermediate geometries along linear isomerization paths were generated for **0**–**3** according to

$$q_i(F) = q_i(0) + \frac{F}{100}[q_i(100) - q_i(0)] \qquad (2)$$

where q_i is a given atomic Cartesian coordinate and F is the fraction of progress along the isomerization coordinate (so that 0 and 100 define the μ-η^1:η^1 and μ-η^2:η^2 peroxo geometries, respectively). We present results in most cases for F values of 0, 20, 40, 60, 80, and 100. Reference to a particular structure along an isomerization coordinate will henceforth be made by adding F as a subscript the structure cardinal, e.g., $\mathbf{2}_{20}$ refers to the structure 20% converted from $\mathbf{2}_0$ to $\mathbf{2}_{100}$. In the cases of systems **2** and **3**, the linear coordinate generates rather high-energy intermediate structures because of the artificial nature of the isomerization (which causes these structures to have very short N–H bonds, for example). In certain cases we elected not to do CASPT2 calculations on such points but instead to focus on the terminal structures. For **0** and **1**, many levels of theory predict the 20% structure to be lower in energy than the 0% congener, suggesting that the raw UB3LYP end-point geometry is not especially representative of the local minimum. However, as our isomerization coordinates are arbitrary and intended only to permit a systematic comparison of methodologies, this is of no particular consequence.

For **4**, geometries were fully optimized in our prior work[28] at both the R and U BLYP/BS4 and B3LYP/BS4 levels. That effort generated not only μ-η^1:η^1 and μ-η^2:η^2 peroxo geometries in the C_i point group but also bis(μ-oxo) geometries in the C_{2h} point group. The natures of all stationary points for **4** were confirmed by calculation of analytic force constants.

Software. Full details on software are provided in the Supporting Information.

Results

$Cu_2O_2{}^{2+}$. The energies for structures of **0** as a function of F were computed at all levels of theory using the BS1 basis set. At the CAS and CASPT2 levels, a large (16,14) active space was employed and the orbitals were optimized for a state average over the first four $^1A_{1g}$ states within the constraints of C_{2h} symmetry. CASPT2 energies were then computed both for the lowest-energy singlet state treated as a single root and for the lowest-energy root of a multistate (MS-CASPT2) treatment including all four roots. While the second and third

TABLE 1: Relative Energies (kcal mol^{-1}) of $\mathbf{0}_F$ Structures with BS1

level of theory	0%	20%	40%	60%	80%	100%
RHF	−47.6	−60.8	−55.9	−39.9	−21.2	0.0
MP2	−3.7	−0.5	8.9	22.3	16.0	0.0
CCSD	−25.8	−28.6	−20.8	−6.8	−0.6	0.0
CCSD(T)	−14.2	−14.2	−5.5	8.1	5.8	0.0
CR-CCSD(T)	−18.6	−19.9	−11.6	2.3	3.1	0.0
CR-CC(2,3),A	−17.4	−18.1	−9.6	4.1	3.2	0.0
CR-CC(2,3),D	−16.5	−17.2	−8.8	4.8	3.9	0.0
CCSD(TQ)	−16.5	−16.4	−7.7	6.0	6.9	0.0
CR-CCSD(TQ)	−18.2	−19.0	−10.6	3.1	3.5	0.0
CR-CC(2,3)+Q[a]	−16.2	−16.4	−7.9	5.6	4.3	0.0
CAS(16,14)	−50.7	−50.3	−41.7	−26.8	−17.7	0.0
CASPT2(16,14)	−7.6	−6.4	2.6	11.5	3.5	0.0
MS-CASPT2(16,14)	−22.5	−19.3	−8.9	3.9	0.0	0.0
BS-BLYP	−25.0	−23.1	−15.0	−6.9	−3.5	0.0
BS-B3LYP	−25.2	−27.4	−21.2	−13.4	−7.8	0.0
BS-mPWPW91	−22.2	−21.7	−14.5	−7.0	−3.8	0.0
BS-mPW1PW91	−24.4	−28.6	−23.3	−15.7	−9.5	0.0
BS-MPW1K	−29.4	−36.8	−32.4	−23.8	−14.5	0.0
BS-TPSS	−19.0	−18.2	−11.2	−4.7	−2.4	0.0
BS-TPSSh	−19.7	−20.8	−14.7	−8.1	−4.7	0.0
sumBS-BLYP	−21.9	−19.5	−10.3	−1.6	0.2	0.0
sumBS-B3LYP	−21.4	−23.2	−16.1	−7.5	−3.2	0.0
sumBS-mPWPW91	−18.9	−18.1	−9.8	−1.8	−0.2	0.0
sumBS-mPW1PW91	−21.0	−24.8	−18.7	−10.2	−4.9	0.0
sumBS-MPW1K	−27.7	−34.9	−29.7	−19.8	−10.3	0.0
sumBS-TPSS	−15.4	−14.1	−6.2	0.6	1.1	0.0
sumBS-TPSSh	−15.8	−16.4	−9.5	−2.5	−0.6	0.0

[a] Computed as CR-CC(2,3),D + {CR-CCSD(TQ) − CR-CCSD(T)}.

roots in the multistate treatment are essentially the same configurations as those determined at the CAS level for all structures, the ground state and state 4 are predicted to mix increasingly strongly as F becomes smaller, leading to a significant decrease in the energy of the end-on isomer relative to that of the side-on at the MS-CASPT2 level compared to single-root CASPT2.

At the DFT level, restricted solutions to the Kohn–Sham SCF equations could not be successfully converged for any structure using the pure functionals BLYP, mPWPW91, and TPSS, although restricted solutions *were* found for the hybrid functionals. However, even those RDFT solutions that could be converged with the hybrid functionals were all unstable to symmetry breaking (computed $\langle S^2 \rangle$ values for the KS determinants ranged from 0.4 to 1.0 depending on structure and functional), so no results are reported for RDFT. Electronic energies, reported relative to those of the side-on $\mathbf{0}_{100}$ structure, are provided in Table 1. Absolute electronic energies, BS-DFT $\langle S^2 \rangle$ values, and $^3B_{2g}$ electronic energies for all structures (the final two quantities are required to compute sumBS-DFT energies) may be found in the Supporting Information.

As we found previously for the case of side-on peroxo versus bis(μ-oxo),[28] there is a very large variation in relative energies as a function of theoretical level. For $\mathbf{0}_0$, a range of roughly 50 kcal mol^{-1} is predicted, although every level does predict the end-on isomer to be lower in energy than the side-on one. Figure 2 graphs the isomerization coordinates predicted by selected levels of theory. Table 1 suggests that the CR-CC results are reasonably well converged with respect to inclusion of higher-order excitations and correlations (cf., the tiny differences between the CR-CCSD(TQ) and CR-CCSD(T) energies and the relatively small differences between the CR-CC(2,3),D and CR-CCSD(T) energies), and based on our prior work with side-on peroxo versus bis(μ-oxo),[28] we anticipate that the CR-CC results,

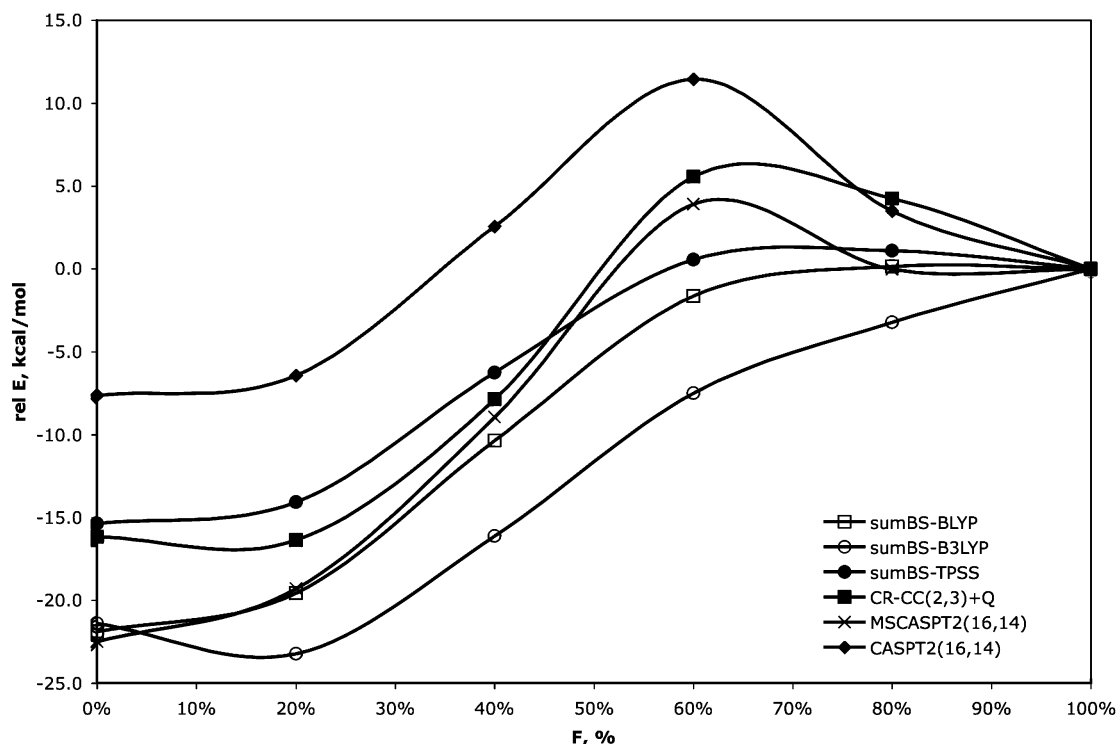**Figure 2.** Relative energy (kcal mol^{-1}) vs F for **0** at select levels of theory (legend inset).

particularly the CR-CC(2,3),D or CR-CC(2,3)+Q curves, may be taken to be an effective standard with which we may evaluate the performance of the other models.

In our prior work,[28] we found that the sumBS predictions of the pure functionals BLYP, mPWPW91, and TPSS were all in good agreement with CR-CC(2,3),D and CR-CC(2,3)+Q (termed CR-CCSD(T)$_L$ and CR-CCSD(TQ)$_L$, respectively, in ref 28). Here, the pure functionals continue to perform well, but there is more variation in their prediction of the energy of **0**$_0$ relative to that of **0**$_{100}$: 6.5 kcal mol^{-1} compared to 3.8 kcal mol^{-1} for side-on peroxo versus bis(μ-oxo).[28] In addition, BLYP was the most accurate functional in our prior work, while here TPSS offers the closest agreement with CR-CC(2,3),D and CR-CC-(2,3)+Q, and BLYP is least good of the pure functionals. The hybrid functionals show a systematic stabilization of **0**$_0$ relative to **0**$_{100}$ with increasing HF exchange.

At the CASSCF level, **0**$_0$ is predicted to be -50.7 kcal mol^{-1} more stable than **0**$_{100}$, which is in very close agreement with the prediction from the single-configurational HF level (-47.6 kcal mol^{-1}). The agreement between the single- and multicon-figurational levels does not, however, arise because the CAS wave functions are nearly single-configurational. On the con-trary, they are all dominated by two nearly equal configurations, consistent with a relatively strong biradical character; the agreement between CASSCF and HF appears merely to reflect an approximately constant error in the single-configurational approximation along the reaction coordinate for the latter method. CASPT2 is predicted strongly to stabilize **0**$_{100}$ relative to **0**$_0$ so that the net stabilization of the latter compared to the former is reduced to -7.6 kcal mol^{-1}, a result which overshoots the CR-CC(2,3),D and CR-CC(2,3)+Q benchmarks. Mixing of the ground state with the fourth singlet root for more end-on like structures in the MS-CASPT2 ansatz brings the reaction coordinate computed at this level into reasonably good agree-ment with CR-CC(2,3),D, CR-CC(2,3)+Q, and TPSS, although there seems to be some remaining overcorrection near the end-on edge of the coordinate.
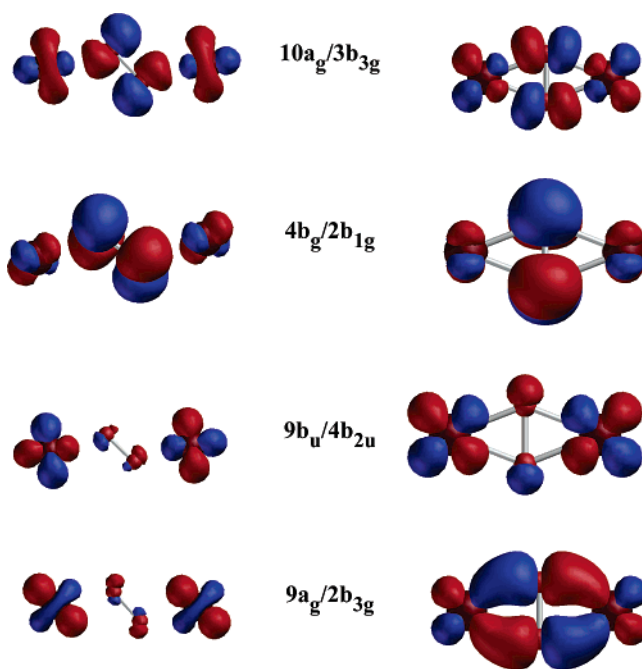

Figure 3. B3LYP/BS1 orbitals for **0**$_0$ (left) and **0**$_{100}$ (right), respectively.

Figure 3 illustrates the nominal 4b$_g$/2b$_{1g}$ HOMO and 10a$_g$/3b$_{3g}$ LUMO orbitals from RB3LYP calculations (which become mixed at the BS-DFT level) for the **0**$_0$ and **0**$_{100}$ structures; the orbitals are labeled according to the different point groups to which their host molecules belong. Also shown in Figure 3 are some other orbitals that are found to be strongly correlated in the post-SCF procedures. Large single-excitation amplitudes (approximately 0.2) from 9a$_g$ to 10a$_g$ are predicted at the CC level along the entire reaction coordinate, increasing slightly at the side-on end. HOMO to LUMO double excitations are also predicted to be large at the CC level, with amplitudes ranging from 0.06 to 0.16 along the reaction coordinate. Double

11562 *J. Phys. Chem. A, Vol. 110, No. 40, 2006*

Cramer et al.

TABLE 2: Relative Energies (kcal mol^{-1}) of 1_F Structures with BS1

level of theory	F					
	0%	20%	40%	60%	80%	100%
CCSD(T)	13.1	10.6	14.1	14.2	7.9	0.0
CR-CCSD(T)	8.3	6.6	11.3	12.8	6.9	0.0
CR-CC(2,3),A	7.2	4.8	8.7	12.4	6.4	0.0
CR-CC(2,3),D	8.6	6.1	10.0	12.6	6.1	0.0
CCSD(TQ)	16.0	15.5	21.0	17.1	9.7	0.0
CR-CCSD(TQ)	7.8	5.9	10.3	13.0	6.9	0.0
CR-CC(2,3)+Q^a	8.2	5.4	9.0	12.7	6.1	0.0
CASPT2(12,12)/4 root	11.3	−2.9	31.2	25.5	15.8	0.0
MS-CASPT2(12,12)/4 root	8.6	0.5	20.5	12.7	5.2	0.0
CASPT2(12,12)/5 root	8.3	24.8	33.9	26.9	20.5	0.0
MS-CASPT2(12,12)/5 root	21.4	24.2	30.4	27.2	16.0	0.0
CASPT2(12,12)/6 root	11.7	21.2	31.5	22.0	16.4	0.0
MS-CASPT2(12,12)/6 root	24.3	32.4	22.5	19.3	26.7	0.0
CASPT2(12,14)/6 root	20.5	31.7	28.8	28.1	32.5	0.0
MS-CASPT2(12,14)/6 root	49.7	−2.2	33.7	26.8	14.5	0.0
CASPT2(16,14)/4 root	37.9	0.3	13.7	4.8	−7.3	0.0
MS-CASPT2(16,14)/4 root	11.3	−2.9	31.2	25.5	15.8	0.0
sumBS-BLYP	−6.6	−8.1	−4.7	0.0	0.8	0.0
sumBS-B3LYP	−1.0	−2.8	−0.3	3.1	3.0	0.0
sumBS-*m*PWPW91	−2.7	−5.1	−2.5	1.3	1.6	0.0
sumBS-*m*PW1PW91	0.0	−2.2	−0.2	2.7	2.5	0.0
sumBS-MPW1K	−4.0	−5.5	−2.6	1.4	2.3	0.0
sumBS-TPSS	0.7	−1.6	0.5	3.3	2.5	0.0
sumBS-TPSSh	2.2	−0.1	1.5	3.9	2.9	0.0

^{a} Computed as CR-CC(2,3),D + {CR-CCSD(TQ) − CR-CCSD(T)}.

excitations from $9b_u$ to the LUMO are also predicted to be important, with amplitudes about half as large as the HOMO/LUMO case. At the CAS level, the occupation numbers of these orbitals reflect the relatively strong biradical character implicit in the CC amplitudes, and the CCSD natural orbital occupation numbers show a similar behavior. Thus, although the molecules are multiconfigurational, there is not a very large change in biradical character predicted as the system isomerizes from end-on to side-on.

Although the isomerization coordinate for **0** belongs to the C_{2h} point group, when that symmetry was used for the CAS calculations, no convergence in relative energies along the coordinate was observed with respect to increasing the active space size to the practical limit of (16,14), even though there is a reasonable, fortuitous agreement between the MS-CASPT2-(16,14) results and the best CR-CC results. Reducing the symmetry to C_i (which permits a greater mixing of the active and inactive orbitals in the CAS) does lead to smooth convergence with larger active spaces but provides energies in very poor agreement with all other predictions (see the Supporting Information).

{(NH$_3$)Cu}$_2$O$_2^{2+}$. The energies for structures of **1** as a function of F were computed at all levels of theory using the BS1 basis set. At the DFT level, restricted solutions to the Kohn−Sham SCF equations could be obtained for all functionals, but they were all unstable to symmetry breaking (computed $\langle S^2 \rangle$ values for the KS determinant ranged from 0.2 to 1.0 depending on structure and functional), so we report only sumBS results in Table 2. The isomerization energetics for select levels of theory are also illustrated graphically in Figure 4.

CAS, CASPT2, and MS-CASPT2 calculations proved problematic for this system. Although the isomerization coordinate for **1** belongs to the C_{2h} point group, when that symmetry was used for the CAS calculations, no convergence in relative energies along the coordinate was observed with respect to increasing the active space size to the practical limit of (16,-14). Moreover, large variations in relative energies were observed when four, five, or six roots were employed in multistate calculations (see Table 2). Interestingly, reducing the symmetry to C_i (which permits a greater mixing of the active and inactive orbitals in the CAS) leads to a smooth convergence and good agreement between active spaces of (12,12), (12,14), and (16,14) and also to good agreement between CASPT2 and MS-CASPT2 (i.e., interactions between multiple roots are rendered negligible). However, the converged energy of 1_0 relative to that of 1_{100} is predicted to be −16.7 kcal mol^{-1}, which is very far from the CR-CC results. Moreover, the PT2
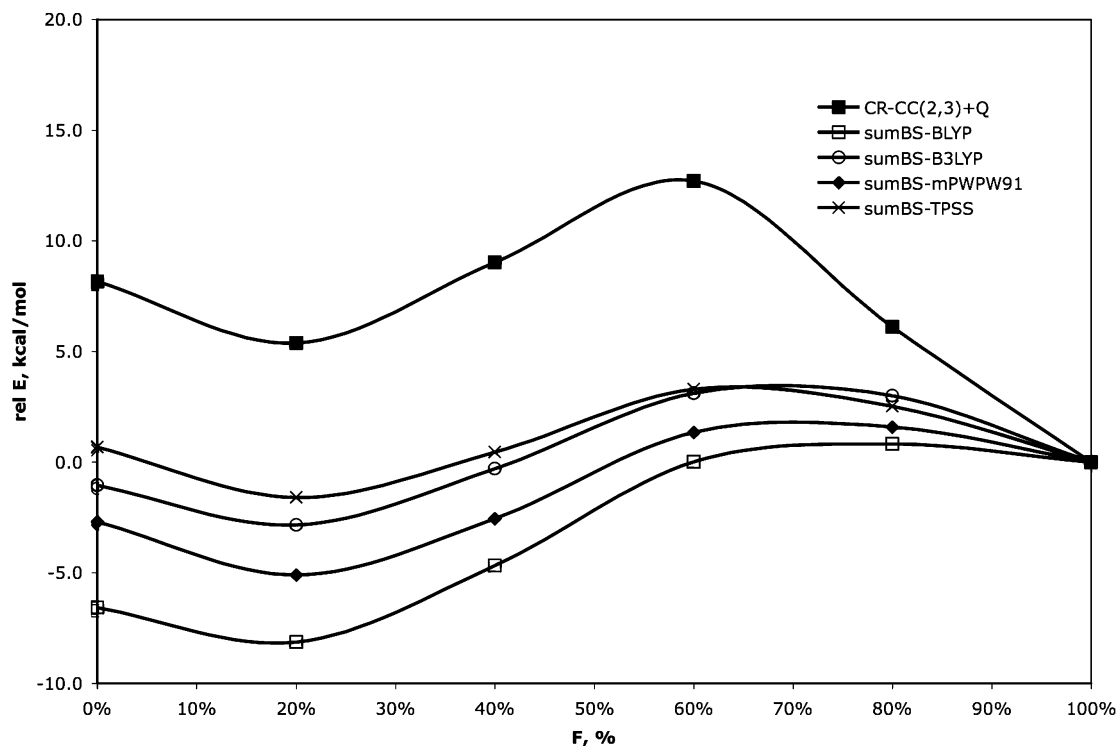

Figure 4. Relative energy (kcal mol^{-1}) vs F for **1** at select levels of theory (legend inset).

Peroxide Coordination in Ligated Cu$_2$O$_2$ Models

J. Phys. Chem. A, Vol. 110, No. 40, 2006 **11563**

TABLE 3: Relative Energies (kcal mol^{-1}) of 2$_F$ Structures with BS1

level of theory	F					
	0%	20%	40%	60%	80%	100%
CCSD(T)	25.3	35.5	67.1	61.4	21.3	0.0
CR-CCSD(T)	24.1	37.6	67.6	61.9	21.3	0.0
CR-CC(2,3),A	18.5	28.3	61.3	58.1	19.9	0.0
CR-CC(2,3),D	20.9	32.0	63.5	59.3	20.3	0.0
CAS(14,13)	73.0					0.0
CASPT2(14,13)	−1.0					0.0
MS-CASPT2(14,13)	−2.6					0.0
sumBS-BLYP	−9.9	8.8	44.4	46.4	16.3	0.0
sumBS-B3LYP	7.9	26.0	56.0	62.3	18.6	0.0
sumBS-*m*PWPW91	−5.4	9.3	41.8	43.0	12.7	0.0
sumBS-*m*PW1PW91	15.1	31.1	57.0	65.8	33.2	0.0
sumBS-MPW1K	30.5	48.6	70.4	86.5	8.6	0.0
sumBS-TPSS	−0.9	14.2	46.8	47.5	16.7	0.0
sumBS-TPSSh	6.6	22.1	52.1	55.3	23.2	0.0

correction for 1$_0$ relative to that of 1$_{100}$ is predicted to be more than −100 kcal mol^{-1}, which can only be regarded with deep suspicion.

As shown in Table 2, the CR-CC results are again well converged with respect to higher-order correlations. For example, no significant differences are observed between the CR-CCSD(T) and CR-CC(2,3),D results, indicating that higher-order terms that are present in CR-CC(2,3),D and absent in CR-CCSD(T) are of limited importance. The effects due to quadruples are small as well, as judged by the small differences between the CR-CCSD(TQ) and CR-CCSD(T) energies. This should be contrasted with the results of the CCSD(T) and CCSD(TQ) calculations, which are quite different from one another, particularly in the middle of the reaction coordinate, suggesting problems with obtaining well-converged results with standard CC methods of the CCSD(T) type. One needs to use CR-CC approaches, particularly the size extensive CR-CC-(2,3),D method, which can handle biradical systems under consideration in an accurate and robust manner. If we take the CR-CC results to be accurate, the DFT results uniformly overestimate the stability of the end-on structure relative to that

of the side-on. Curiously, the effect of including HF exchange is variable. With small amounts of HF exchange, the energy of 1$_0$ relative to that of 1$_{100}$ increases, improving agreement with CR-CC; this is true for B3LYP versus BLYP, *m*PW1PW91 versus *m*PWPW91, and TPSSh versus TPSS. However, this trend evidently reverses as MPW1K, with the largest amount of HF exchange, predicts 1$_0$ to be more stable relative to 1$_{100}$ than the pure *m*PWPW91 functional from which it derives.

{(NH$_3$)$_2$Cu}$_2$O$_2$$^{2+}$. The energies for structures of **2** as a function of *F* were also computed at all levels of theory using the BS1 basis set except that consideration of quadruple excitations was no longer practical at the CC levels (Table 3). At the CAS, CASPT2, and MS-CASPT2 levels, a (14,13) active space was chosen accounting for four singlet roots and only the *F* = 0 and *F* = 100 structures were considered. We note that the reaction coordinate for **2** now belongs to the *C$_i$* point group, so that is the natural choice for the CAS calculations.

At the DFT level, restricted solutions to the Kohn−Sham SCF equations could be obtained for all functionals. With the pure DFT functionals, the RDFT solutions for *F* = 100 were stable to spin-symmetry breaking but others were not, so we continue to consider only results from the sumBS-DFT protocol. Absolute electronic energies, BS-DFT ⟨*S*^{2}⟩ values, and triplet electronic energies for all structures at all levels of theory are provided in the Supporting Information.

As in prior systems, the CR-CC results appear to have achieved a good level of convergence by the point at which CR-CC(2,3),D is reached. Also as in prior systems considered within the constraints of *C$_i$* symmetry, the CAS, CASPT2, and MS-CASPT2 levels are all observed to be well converged with respect to active space size by the time (14,13) is reached. However, as also observed for the prior systems, the PT2 correction for the *F* = 0 structure is enormous and drastically overstabilizes that structure. Mixing with higher roots has negligible effect on the system.

The DFT results also follow some prior trends. First, the pure functionals all predict the highest stability of **2**$_0$ relative to **2**$_{100}$,
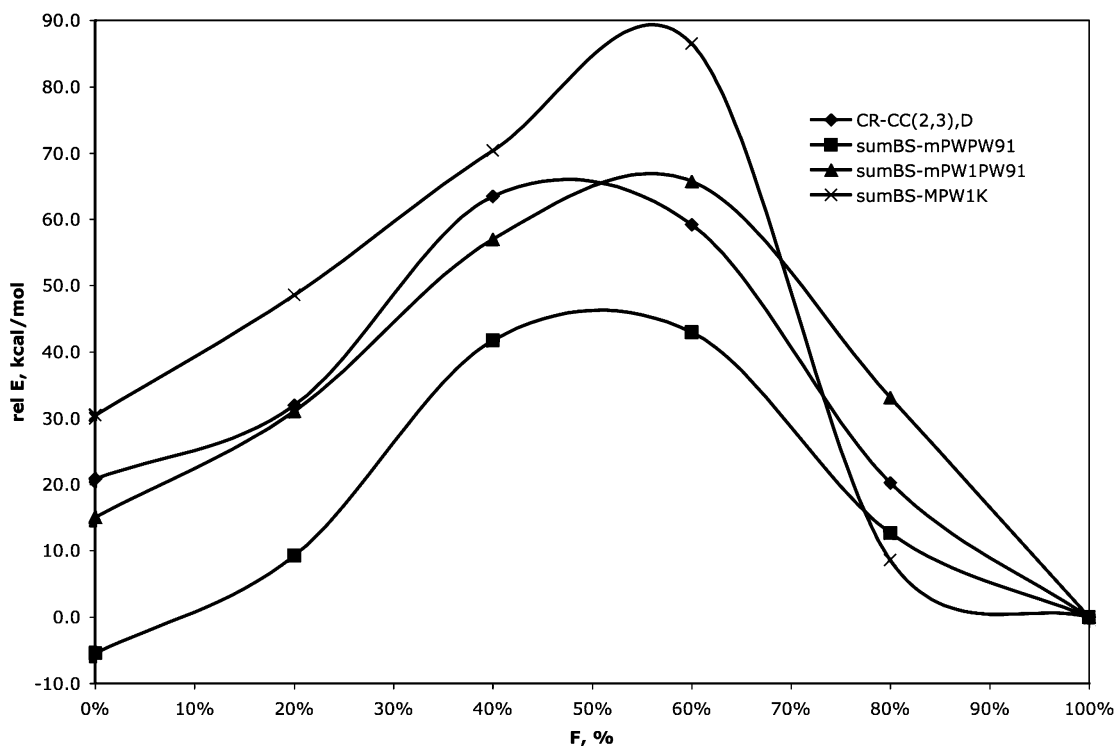

Figure 5. Relative energy (kcal mol^{-1}) vs *F* for **2** at select levels of theory (legend inset).

11564 *J. Phys. Chem. A, Vol. 110, No. 40, 2006*

Cramer et al.

TABLE 4: Relative Energies (kcal mol^{-1}) of 3_F Structures with BS1 unless Otherwise Noted

level of theory	0%	20%	40%	60%	80%	100%
CCSD(T)	23.4	30.1	45.5	37.7	15.7	0.0
CR-CCSD(T)	30.4	34.4	45.9	35.5	13.9	0.0
CR-CC(2,3),D/BS2	23.8	27.4	40.3	30.5	10.4	0.0
CR-CC(2,3),D^a	26.6	30.6	42.2	33.2	13.1	0.0
CAS(16,14)	99.0					0.0
CASPT2(16,14)	39.4					0.0
MS-CASPT2(16,14)	38.7					0.0
sumBS-BLYP	1.0	9.8	24.1	23.1	8.1	0.0
BS-B3LYP	8.7	13.4	25.9	27.7	16.5	0.0
sumBS-B3LYP	22.9	27.8	39.5	37.6	22.5	0.0
sumBS-mPWPW91	3.1	8.6	20.9	19.8	6.0	0.0
sumBS-mPW1PW91	30.3	31.9	41.7	39.9	25.6	0.0
sumBS-MPW1K	53.9	52.4	60.7	59.6	45.2	0.0
sumBS-TPSS	7.1	12.8	24.8	23.0	8.0	0.0
sumBS-TPSSh	17.4	21.6	32.5	30.7	15.6	0.0

^{a} Computed as CR-CCSD(T)/BS1 + {CR-CC(2,3),D/BS2 − CR-CCSD(T)/BS2}.

but they are only in modestly good agreement with one another, with BLYP predicting the largest stability for 2_0, followed by mPWPW91, followed by TPSS. Increased HF exchange increases the energy of 2_0 relative to that of 2_{100}, and that trend is now consistent throughout the range of HF exchange spanned from pure mPWPW91 to 48.2% HF-including MPW1K (although, oddly, the trend does reverse for 2_{80} relative to 2_{100}). As shown in Figure 5, mPW1PW91, with 25% HF exchange, gives fairly good agreement with CR-CC(2,3),D, although clearly there seems to be no way to know in advance what amount of HF exchange may be appropriate in any of the systems studied thus far.

Note that the high barrier predicted by all of the methods for the isomerization is purely an artifact of the linear coordinate chosen. However, as the system is designed primarily to test methodologies and not to mimic any well-characterized experimental molecule, this issue is not important. What is, perhaps, more interesting is that the mPW1PW91 and CR-C(2,3),D

TABLE 5: Relative Energies (kcal mol^{-1}) of Isomers of 4 with BS4^a

level of theory	4a	4b	4c
BLYP	8.3	0.0	−0.2 (−1.6)^b
B3LYP	27.3	0.0 (−0.4)^b	17.2 (12.3)^b

^{a} The energies for **4c** at the BLYP level and for **4b** and **4c** at the B3LYP level are sumBS energies (other cases have stable restricted solutions). ^{b} Relative sumBS energy computed for the structure optimized at the RDFT level of theory.

isomerization curves shown in Figure 5, which are obtained using exactly the same set of nuclear geometries, are very close to one another.

{(NH$_3$)$_3$Cu}$_2$O$_2^{2+}$. Energies for **3** were computed at all levels of theory using the BS1 basis set, except that (i) the incremental changes on going from the CR-CCSD(T) to CR-CC(2,3) levels were computed with the BS2 basis set and (ii) consideration of quadruple excitations was not practical at the CC levels. At the CAS, CASPT2, and MS-CASPT2 levels, a (16,14) active space and four roots were employed within the constraints of C_i symmetry. As with all other systems in this point group, results were observed to be well converged with respect to those of somewhat smaller active spaces. At the DFT level, only select $F = 100$ structures had SCF solutions that were stable to spin-symmetry breaking at the RDFT level, so we continue to consider only sumBS energies, except that the raw BS-B3LYP results are also reported for comparison. Representative relative energies are provided in Table 4, and absolute electronic energies, BS-DFT ⟨S^2⟩ values, and triplet electronic energies for all structures at all levels of theory are in the Supporting Information.

Trends in this instance are quite similar to those already noted above for **2**. CR-CC seems well converged, CASPT2 is well converged but behaves erratically for the $F = 0$ isomer (in this context, it is worth noting that the CAS and CASPT2 results for $F = 100$ are essentially identical whether C_i or C_{2h} symmetry is used, so the variation in relative energy observed for $F = 0$ is truly associated with that structure), and coordinates computed
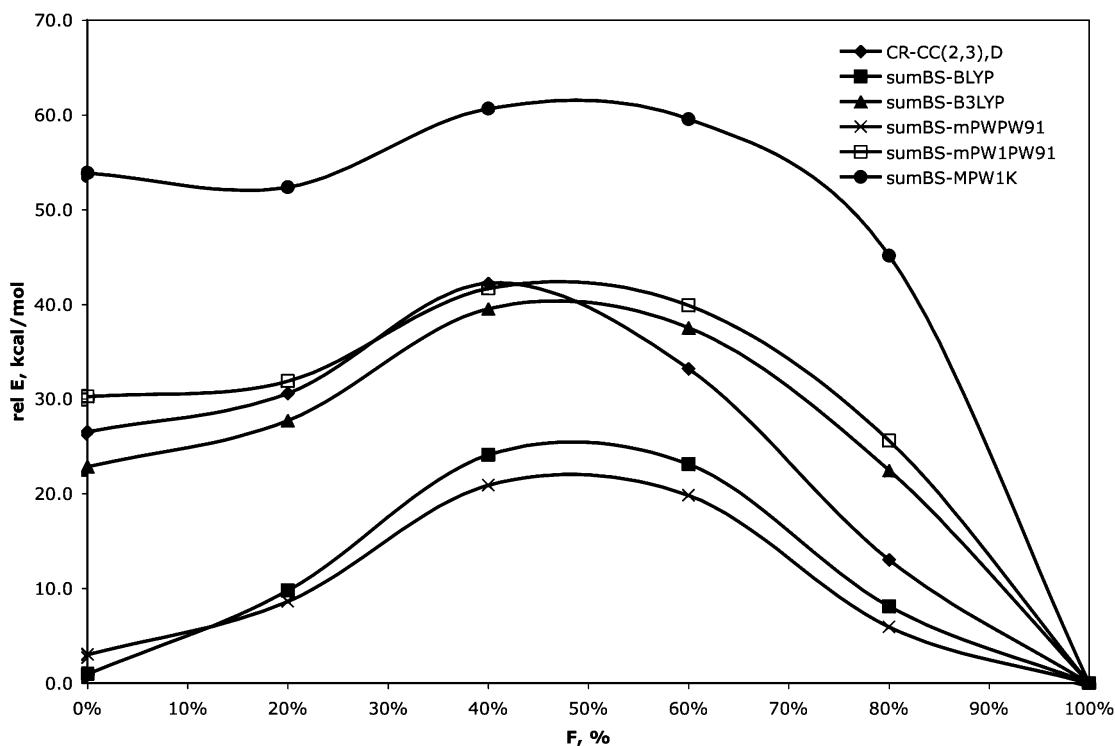

Figure 6. Relative energy (kcal mol^{-1}) vs F for **3** at select levels of theory (legend inset).

Peroxide Coordination in Ligated Cu$_2$O$_2$ Models

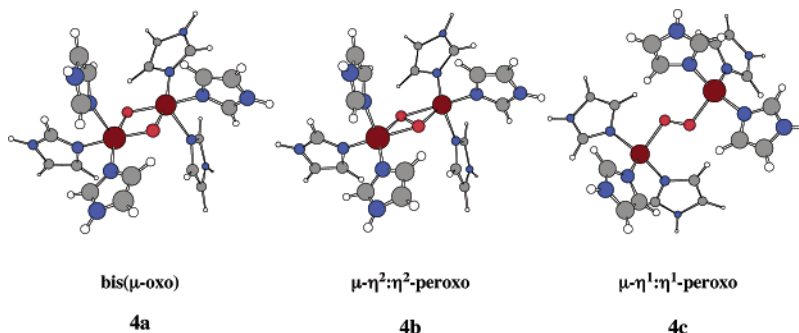*J. Phys. Chem. A, Vol. 110, No. 40, 2006* **11565**

Figure 7. Structures optimized at the BLYP/BS4 level of theory (B3LYP structures are qualitatively similar; all structures belong to the C_i point group).

TABLE 6: Selected Energies (kcal mol^{-1}) Relative to μ-η^2:η^2 Peroxo as a Function of Basis Set and Theoretical Level

structure	BS-BLYP	CR-CC(2,3),D	CASPT2(14,13)[a]
0			
bis(μ-oxo)	36.0/ 32.4/ 32.4[b]	35.5/ 44.4/ 42.4	29.3/ 46.0/ 34.4
μ-η^1:η^1 peroxo	−25.0/−31.3/−32.6	−16.5/−29.5/−24.7	−46.1/−56.7/−40.3
1			
bis(μ-oxo)	34.0/ 34.7/ 36.1	30.6/ 33.6/ 34.9	
μ-η^1:η^1 peroxo	−10.8/−11.0/−11.7	8.6/ −0.6/ 1.1	
3			
bis(μ-oxo)	8.4/ 9.3/ 9.9		
μ-η^1:η^1 peroxo	−3.5/ −4.0/ −4.6		

[a] Based on CAS wave functions not constrained to be symmetric. [b] Results are BS1/BS1d/BS1t.

at DFT levels destabilize structures with $F < 100$ proportional to the amount of HF exchange included in the functional. In the case of **3**, the *m*PW1PW91 and B3LYP functionals both show reasonable agreement with CR-CC(2,3),D (see Figure 6). As in **0**−**2**, analysis of CAS orbital occupation numbers and CC amplitudes suggests that both end-on and side-on isomers may be regarded as Cu(II)/Cu(II) singlet systems with a relatively large degree of biradical character.

{(Imid)$_3$Cu}$_2$O$_2^{2+}$. In our prior work[28] we optimized bis(μ-oxo) (**4a**), μ-η^2:η^2 peroxo (**4b**), and μ-η^1:η^1 peroxo (**4c**) isomers at the BLYP and B3LYP levels of theory (Figure 7). BLYP was chosen based on its excellent performance for the prediction of the isomerization energetics of **0**−**3** along a reaction coordinate from bis(μ-oxo) to side-on peroxo, while B3LYP was chosen because of its substantial prior use for the modeling of dicopper−dioxo systems.[92−98] Full details are provided in our prior work, and we simply recapitulate the relative energetics here in Table 5. B3LYP predicts the μ-η^2:η^2 peroxo isomer **4b** to be more stable than the bis(μ-oxo) isomer **4a** by about a 20 kcal mol^{-1} larger margin than does BLYP. The same is true for the energy of **4c** relative to that of **4a**: the B3LYP prediction is about 17 kcal mol^{-1} larger than that of BLYP. We note that the energy of the end-on structure optimized using *restricted* B3LYP is predicted to be about 5 kcal mol^{-1} more stable than that of the analogous structure optimized with raw *unrestricted* B3LYP, again reflecting the rather poor quality of end-on peroxo structures predicted at the UB3LYP level (cf., the generally greater stability of 20% structures compared to 0% structures predicted by most levels of theory for **0** and **1**). With the BLYP functional the RBLYP structure for **4c** is also lower in energy than the UBLYP structure, but by a much smaller amount, 1.4 kcal mol^{-1} versus 4.9 kcal mol^{-1} for B3LYP.

Basis Set Effects. The effects of using an all-electron basis set for copper compared to an effective core potential were examined by comparing BS-BLYP, CR-CC(2,3),D, and CASPT2-(14,13) calculations with the BS1, BS1d, and BS1t basis sets (Table 6). In addition to being all-electron in nature, the BS1d

and BS1t basis sets also improve on the valence and polarization functions available to copper. For these calculations, we considered not only the μ-η^1:η^1 and μ-η^2:η^2 peroxo isomers but also the corresponding bis(μ-oxo) isomers.

For system **0**, all levels of theory show a significant degree of sensitivity to the basis set. In general, on going from BS1 to BS1d the energies of the bis(μ-oxo) and μ-η^1:η^1 peroxo isomers increase and decrease, respectively, relative to those of the μ-η^2:η^2 peroxo isomer by as much as 17 kcal mol^{-1}. The CASPT2 level shows the greatest sensitivity, the CR-CC(2,3),D level a reduced degree, and the BS-BLYP level is much less sensitive, consistent with the usual observations vis a vis the sensitivity of DFT energies to basis set size. Increasing the basis set further from BS1d to BS1t in most instances moves the relative energies back closer to the original BS1 values, which may indicate that the greater flexibility in the BS1t valence and polarization space is providing opportunities for additional core correlation included in the pseudopotential by construction. The bis(μ-oxo) energies obtained in the BS-BLYP and CR-CC(2,3),D calculations are less sensitive to the basis set than the energies of the μ-η^1:η^1 peroxo isomer. However, none of the main conclusions regarding the relative energetics of the three isomers considered in Table 6 are affected by the basis set choice.

As the various levels are subject, for the most part, to qualitatively similar basis set effects, comparisons between them are valid independent of basis set. However, no definitively quantitative prediction of the actual relative energetics for **0** is really possible. Of course, **0** is a rather unusual system as it lacks any ligands on copper beyond the oxygen atoms. For **1**, calculations at the BS-BLYP and CR-CC(2,3),D levels reveal the basis set sensitivity to be qualitatively similar to **0**, but substantially reduced in magnitude, suggesting that demands on basis set completeness are reduced as a more typical ligand environment is constructed around the copper atoms. Indeed, for **3** the size of the system permits this point to be evaluated only at the BS-BLYP level, but the basis set effects are predicted to span a range of less than 2 kcal mol^{-1} for this congener.
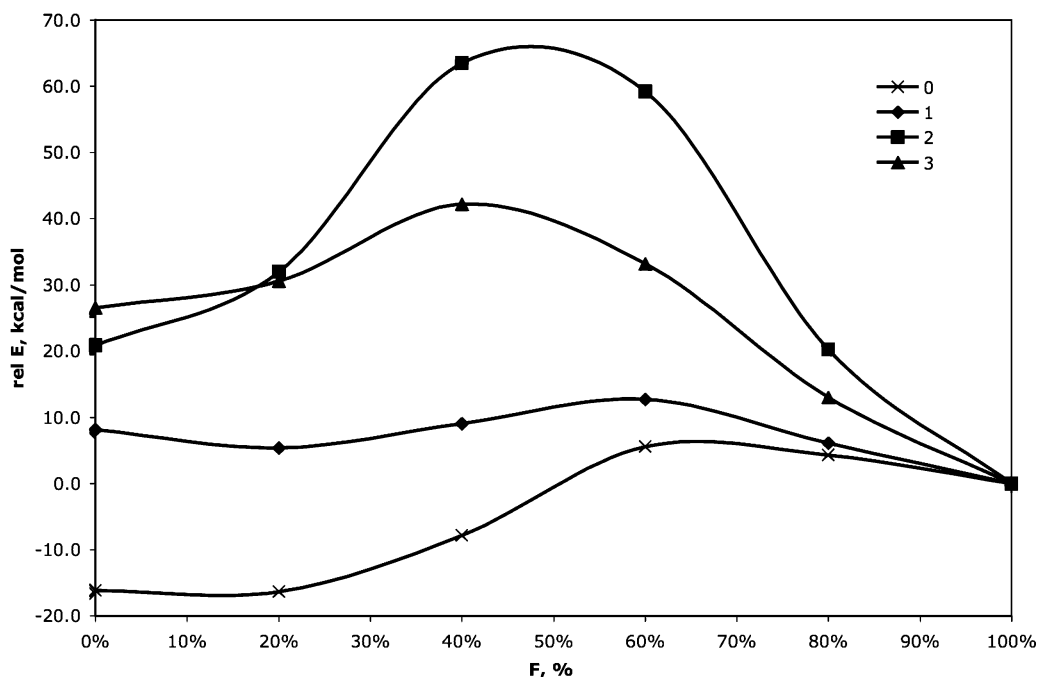
Figure 8. Relative energy (kcal mol^{-1}) vs F for **0**−**3** at best CR-CC levels of theory (see legend insets in Figures 2, 4, 5, and 6 and data in Tables 1−4).

Discussion

A first question that arises in the analysis of the above results is the degree to which the CR-CC data should be considered to be an adequate standard against which to compare other methods. Experimental data for the end-on to side-on equilibrium are almost nonexistent, and indeed end-on species have only been definitively characterized with tetradentate ligands that are large and complex (attempts to model a system with four ammonia ligands on each copper were not successful because the end-on species is unstable to dissociation into molecular oxygen and two Cu(NH$_3$)$_4$$^+$ cations). However, there are a number of arguments that may be marshalled in support of CR-CC as a standard. First, it appears to be reasonably well converged with respect to inclusion of high-order correlations and accounting for size extensivity. Second, it has been demonstrated to provide good descriptions of biradicals in organic systems.[74−76] Third, and importantly, it *does* agree with other key levels of theory and experimental analogues in its predictions for the equilibrium between bis(μ-oxo) and side-on peroxo forms.[28] And finally, if we consider the CR-CC predictions for the end-on/side-on equilibrium as a function of the number of ligands, the trend is intuitively reasonable (Figure 8). In the unligated system, there is strong Coulombic repulsion between the two copper cations, and that repulsion is reduced in the end-on structure where they are nearly 5 Å apart compared to 3.6 Å in the side-on case. As ammonia ligands are added to the copper atoms, ligand-to-metal charge-transfer reduces the Coulomb repulsion and permits differences in covalent interactions between the copper and oxygen atoms in the two forms to influence the equilibrium. The side-on structure, with its η^2 coordination of the O$_2$ ligand, has increased such interactions and becomes increasingly more stable with additional ammonia ligands. This effect appears to be nearly saturated with the addition of the third ammonia ligand judging from the small change in the end-on/side-on energy difference on going from **2** to **3** (recall also that the significant barriers for the isomerization of **2** and **3** are artifacts of the linear isomerization coordinate). This analysis is consistent with the observation that

long-lived end-on geometries have only been observed experimentally with tetradentate ligands that present coordination options to the copper atoms that are improved over η^2 coordination to O$_2$.

With respect to the other levels of theory, it is difficult to understand the precise reasons for the failure of CASPT2, MS-CASPT2, and DFT to perform in a consistent fashion. With respect to DFT, there is nearly always some functional that agrees reasonably well with the CR-CC model, but obtaining that agreement requires that the percentage of HF exchange included in the functional be tuned precisely right, with little guidance provided before the fact on how to choose that percentage. This is in contrast to the bis(μ-oxo)/side-on peroxo equilibrium, where pure functionals outperform hybrid functionals for every case of **0**−**3**.[28] We previously rationalized that behavior as deriving from some cancellation of errors in the degree to which strongly varying dynamical and nondynamical correlation along the bis(μ-oxo)/side-on peroxo reaction coordinate were accounted for by the pure functionals, which tend to resist breaking spin-symmetry until biradical character becomes quite high. By contrast, the end-on/side-on peroxo reaction coordinate seems to have a reasonably constant degree of nondynamical correlation—both endpoints are fairly pure biradicals—and all solutions are broken symmetry. Evidently, however, remaining variations in character are sufficient to affect functional performance but not in a systematic way that appears to be correlated with any easily identified feature that is a function of the ligation number.

With respect to the CASPT2 and MS-CASPT2 models, there is the curious observation that results obtained within the constraints of C_i symmetry are very consistent. The $F = 0$ structure is predicted to be vastly higher in energy at the CAS level, the CASPT2 level predicts an enormous (over)correction, and mixing of excited states in the MS-CASPT2 procedure does not seem to be important for the lowest-energy root. However, in **0** and **1** where C_{2h} symmetry can be exploited, such behavior is not observed with the C_{2h} solutions. Instead, reasonable agreement with CR-CC results can be obtained, but

demonstrating convergence with respect to active space size and the number of roots included in the MS-CASPT2 treatment is not possible.

It appears that a more thorough understanding of the nature of the excited singlet (and possibly triplet) states would be helpful in better understanding the Cu_2O_2 system in general. Such a study is not trivial given the issues raised here, and other levels of theory that might be employed, e.g., TDDFT or equation-of-motion CC (EOMCC) approaches, will also be faced with challenges associated with the biradical character of the ground states that would typically be chosen as reference states. Nevertheless, it seems likely that further theoretical progress on this important structural motif will require movement in this direction. The recently developed extensions of CR-CC to excited states, in which EOMCCSD energies are corrected for the effects of triples (the CR-EOMCCSD(T) approaches)[67,99] may prove useful in this context.

Last, we consider the implication of the present results, together with those from our previous work, for the modeling of experimentally relevant Cu_2O_2 chemistry. Our current calculations are especially relevant to previously reported work of Metz and Solomon,[100] who studied a constrained reaction coordinate for the binding of molecular (triplet) O_2 to a deoxyhemocyanin model in which the imidazole ligands of the enzyme active site were replaced by ammonia. This corresponds exactly to our system **3**. Metz and Solomon described a process whereby initial binding occurs in an end-on fashion, followed by a low-barrier conversion to a side-on peroxo with concomitant intersystem crossing to the singlet state. Based on spectroscopic calibration, they chose to model this process with the B3LYP functional, and they emphasized the importance of employing a sumBS energy correction. As noted in Table 4 and Figure 6, sumBS-B3LYP shows excellent agreement with CR-CC(2,3),D for system **3**, so our results support the validity of the energetics described by Metz and Solomon.

Interestingly, raw BS-B3LYP (i.e., no sum method correction for spin contamination) does rather poorly for **3** (Table 4), predicting the end-on peroxo to be about 14 kcal mol^{-1} more stable relative to the side-on isomer than is predicted at the CR-CC(2,3),D and sumBS-B3LYP levels. If we compare Tables 4 and 5, we see that predictions for systems **3** and **4** are quantitatively similar, suggesting only a minor influence for ammonia versus imidazole as a ligand, at least for the isomerization energetics. This observation is important insofar as one might otherwise question whether our general observations with ammonia as a ligand would extend to more realistic, large, and possibly multidentate ligands.

Continuing with the comparison of results in Tables 4 and 5, given that the pure functional (sumBS-)BLYP does rather poorly in the prediction of the side-on/end-on peroxo equilibrium for **3** (by comparison to CR-CC(2,3),D), and given that hybrid sumBS-B3LYP does quite well, this suggests that our best prediction for **4** is that the end-on peroxo isomer is $12-17$ kcal mol^{-1} less stable than the side-on peroxo case. Again consistent with results for **3**, we find that the raw BS-B3LYP prediction is for end-on peroxo to be only $2-3$ kcal mol^{-1} less stable than the side-on isomer, i.e., a difference of about 14 kcal mol^{-1} (data in the Supporting Information).

This has potential implications for the modeling of systems such as tyrosinase. For example, Siegbahn and co-workers have described comprehensive studies of several paths for a side-on peroxo species coordinated by six imidazole ligands reacting with either phenol or phenolate.[94,96,97] At the raw BS-B3LYP level, phenolate coordination to one copper atom is reported to

induce a distortion of the side-on μ-η^2:η^2 peroxo species to a μ-η^2:η^1 geometry that is intermediate between end-on and side-on. Subsequently, this species either initiates electrophilic aromatic substitution or it further decoordinates to a μ-η^2:η^0 peroxyl radical that may be the reactive species.[96] We have not explored μ-η^2:η^1 or μ-η^2:η^0 geometries here, but given our results for the fully end-on μ-η^1:η^1 geometry, it would be interesting to assess the degree to which application of the sumBS method might affect the relevant molecular energetics of such geometries.

The combination of this work with our prior study[28] on the bis(μ-oxo)/side-on peroxo equilibrium suggests that the modeling of potential energy surfaces associated with Cu_2O_2 cores is fraught with peril when the goal is to include a variety of coordination motifs. As such, we anticipate that our results will prove useful for the evaluation of newly developed wave function and density functional models. It is encouraging to observe that the CR-CC approaches, particularly the recently developed size extensive CR-CC(2,3),D model, provide reasonable results, both for the previously studied[28] bis(μ-oxo)/side-on peroxo equilibrium, where one needs to balance biradical and closed-shell regions of the potential energy surface, and the end-on/side-on equilibrium considered in this work, where both limiting structures have significant degrees of biradical character. This prompts the development of low-order scaling (e.g., local) variants of the CR-CC methods and parallel CR-CC codes that might be applied to imidazole and other ligands larger than ammonia.

Supporting Information Available: Cartesian coordinates, absolute (singlet and triplet) and relative electronic energies at all levels of theory for all structures, BS-DFT $\langle S^2 \rangle$ values, and additional technical details on software. This material is available free of charge via the Internet at http://pubs.acs.org.

References and Notes

(1) Solomon, E. I.; Baldwin, M. J.; Lowery, M. D. *Chem. Rev.* **1992**, *92*, 521.

(2) Kitajima, N.; Moro-oka, Y. *Chem. Rev.* **1994**, *94*, 737.

(3) Fox, S.; Karlin, K. D. In *Active Oxygen in Biochemistry*; Valentine, J. S., Foote, C. S., Greenberg, A., Liebman, J. F., Eds.; Blackie Academic & Professional, Chapman & Hall: Glasgow, Scotland, 1995; p 188.

(4) Kaim, W.; Rall, J. *Angew. Chem., Int. Ed. Engl.* **1996**, *35*, 43.

(5) Klinman, J. P. *Chem. Rev.* **1996**, *96*, 2541.

(6) Solomon, E. I.; Sundaram, U. M.; Machonkin, T. E. *Chem. Rev.* **1996**, *96*, 2563.

(7) Solomon, E. I.; Chen, P.; Metz, M.; Lee, S.-K.; Palmer, A. E. *Angew. Chem., Int. Ed.* **2001**, *40*, 4570.

(8) Gamez, P.; Koval, I. A.; Reedijk, J. *Dalton Trans.* **2004**, 4079.

(9) Decker, H.; Dillinger, R.; Tuczek, F. *Angew. Chem., Int. Ed.* **2000**, *39*, 1591.

(10) Solomon, E. I.; Tuczek, F.; Root, D. E.; Brown, C. A. *Chem. Rev.* **1994**, *94*, 827.

(11) Tolman, W. B. *Acc. Chem. Res.* **1997**, *30*, 227.

(12) Mirica, L. M.; Ottenwaelder, X.; Stack, T. D. P. *Chem. Rev.* **2004**, *104*, 1013.

(13) Lewis, E. A.; Tolman, W. B. *Chem. Rev.* **2004**, *104*, 1047.

(14) Cole, A. P.; Mahadevan, V.; Mirica, L. M.; Ottenwaelder, X.; Stack, T. D. P. *Inorg. Chem.* **2005**, *44*, 7345.

(15) Shearer, J.; Zhang, C. X.; Zakharov, L. N.; Rheingold, A. L.; Karlin, K. D. *J. Am. Chem. Soc.* **2005**, *127*, 5469.

(16) Hatcher, L. Q.; Vance, M. A.; Sarjeant, A. A. N.; Solomon, E. I.; Karlin, K. D. *Inorg. Chem.* **2006**, *45*, 3004.

(17) Tolman, W. B. *J. Biol. Inorg. Chem.* **2006**, *11*, 261.

(18) Hatcher, L. Q.; Karlin, K. D. In *Advances In Inorganic Chemistry*; van Eldik, R., Reedijk, J., Eds.; Academic Press: New York, 2006; Vol. 58, p 131.

(19) Stack, T. D. P. *Dalton Trans.* **2003**, 1881.

(20) Jacobson, R. R.; Tyeklar, Z.; Farooq, A.; Karlin, K. D.; Liu, S.; Zubieta, J. *J. Am. Chem. Soc.* **1988**, *110*, 3690.

(21) Henson, M. J.; Vance, M. A.; Zhang, C. X.; Liang, H. C.; Karlin, K. D.; Solomon, E. I. *J. Am. Chem. Soc.* **2003**, *125*, 5186.

(22) Yamaguchi, S.; Wada, A.; Funahashi, Y.; Nagatomo, S.; Kitagawa, T.; Jitsukawa, K.; Masuda, H. *Eur. J. Inorg. Chem.* **2003**, 4378.

(23) Weitzer, M.; Schindler, S.; Brehm, G.; Schneider, S.; Hormann, E.; Jung, B.; Kaderli, S.; Zuberbuhler, A. D. *Inorg. Chem.* **2003**, *42*, 1800.

(24) Hatcher, L. Q.; Karlin, K. D. *J. Biol. Inorg. Chem.* **2004**, *9*, 669.

(25) Minami, K.; Mizuta, M.; Suzuki, M.; Aizawa, T.; Arai, K. *Phys. Chem. Chem. Phys.* **2006**, *8*, 2257.

(26) Mizuno, M.; Hayashi, H.; Fujinami, S.; Furutachi, H.; Nagatomo, S.; Otake, S.; Uozumi, K.; Suzuki, M.; Kitagawa, T. *Inorg. Chem.* **2003**, *42*, 8534.

(27) Jung, B.; Karlin, K. D.; Zuberbühler, A. D. *J. Am. Chem. Soc.* **1996**, *118*, 3763.

(28) Cramer, C. J.; Wloch, M.; Piecuch, P.; Puzzarini, C.; Gagliardi, L. *J. Phys. Chem. A* **2006**, *110*, 1991.

(29) Cahoy, J.; Holland, P. L.; Tolman, W. B. *Inorg. Chem.* **1999**, *38*, 2161.

(30) Holland, P. L.; Tolman, W. B. *Coord. Chem. Rev.* **1999**, *192*, 855.

(31) Pidcock, E.; DeBeer, S.; Obias, H. V.; Hedman, B.; Hodgson, K. O.; Karlin, K. D.; Solomon, E. I. *J. Am. Chem. Soc.* **1999**, *121*, 1870.

(32) Liang, H.-C.; Zhang, C. X.; Henson, M. J.; Sommer, R. D.; Hatwell, K. R.; Kaderli, S.; Zuberbühler, A. D.; Rheingold, A. L.; Solomon, E. I.; Karlin, K. D. *J. Am. Chem. Soc.* **2002**, *124*, 4170.

(33) Que, L.; Tolman, W. B. *Angew. Chem., Int. Ed.* **2002**, *41*, 1114.

(34) Liang, H. C.; Henson, M. J.; Hatcher, L. Q.; Vance, M. A.; Zhang, C. X.; Lahti, D.; Kaderli, S.; Sommer, R. D.; Rheingold, A. L.; Zuberbuhler, A. D.; Solomon, E. I.; Karlin, K. D. *Inorg. Chem.* **2004**, *43*, 4115.

(35) Dolg, M.; Wedig, U.; Stoll, H.; Preuss, H. *J. Chem. Phys.* **1987**, *86*, 866.

(36) Pierloot, K.; Dumez, B.; Widmark, P.-O.; Roos, B. O. *Theor. Chim. Acta* **1995**, *90*, 87.

(37) Hehre, W. J.; Radom, L.; Schleyer, P. v. R.; Pople, J. A. *Ab Initio Molecular Orbital Theory*; Wiley: New York, 1986.

(38) Easton, R. E.; Giesen, D. J.; Welch, A.; Cramer, C. J.; Truhlar, D. G. *Theor. Chim. Acta* **1996**, *93*, 281.

(39) Roos, B. O.; Lindh, R.; Malmqvist, P. A.; Veryazov, V.; Widmark, P. O. *J. Phys. Chem. A* **2005**, *109*, 6575.

(40) Becke, A. D. *Phys. Rev. A* **1988**, *38*, 3098.

(41) Lee, C.; Yang, W.; Parr, R. G. *Phys. Rev. B* **1988**, *37*, 785.

(42) Perdew, J. P. In *Electronic Structure of Solids '91*; Ziesche, P., Eschrig, H., Eds.; Akademie Verlag: Berlin, 1991; p 11.

(43) Perdew, J.; Wang, Y. *Phys. Rev. B* **1992**, *45*, 13244.

(44) Adamo, C.; Barone, V. *J. Chem. Phys.* **1998**, *108*, 664.

(45) Tao, J.; Perdew, J. P.; Staroverov, V. N.; Scuseria, G. E. *Phys. Rev. Lett.* **2003**, *91*, 146401.

(46) Becke, A. D. *J. Chem. Phys.* **1993**, *98*, 5648.

(47) Stephens, P. J.; Devlin, F. J.; Chabalowski, C. F.; Frisch, M. J. *J. Phys. Chem.* **1994**, *98*, 11623.

(48) Lynch, B. J.; Fast, P. L.; Harris, M.; Truhlar, D. G. *J. Phys. Chem. A* **2000**, *104*, 4811.

(49) Staroverov, V. N.; Scuseria, G. E.; Tao, J.; Perdew, J. P. *J. Chem. Phys.* **2003**, *119*, 12129.

(50) Cramer, C. J. *Essentials of Computational Chemistry: Theories and Models*, 2nd ed.; John Wiley & Sons: Chichester, U.K., 2004.

(51) Ziegler, T.; Rauk, A.; Baerends, E. J. *Theor. Chim. Acta* **1977**, *43*, 261.

(52) Yamaguchi, K.; Jensen, F.; Dorigo, A.; Houk, K. N. *Chem. Phys. Lett.* **1988**, *149*, 537.

(53) Lim, M. H.; Worthington, S. E.; Dulles, F. J.; Cramer, C. J. In *Chemical Applications of Density Functional Theory*; Laird, B. B., Ross, R. B., Ziegler, T., Eds.; American Chemical Society: Washington, DC, 1996; Vol. 629, p 402.

(54) Isobe, H.; Takano, Y.; Kitagawa, Y.; Kawakami, T.; Yamanaka, S.; Yamaguchi, K.; Houk, K. N. *Mol. Phys.* **2002**, *100*, 717.

(55) Gräfenstein, J.; Cremer, D. *Mol. Phys.* **2001**, *99*, 981.

(56) Čížek, J. *J. Chem. Phys.* **1966**, *45*, 4256.

(57) Čížek, J. *Adv. Chem. Phys.* **1969**, *14*, 35.

(58) Purvis, G. D.; Bartlett, R. J. *J. Chem. Phys.* **1982**, *76*, 1910.

(59) Scuseria, G. E.; Scheiner, A. C.; Lee, T. J.; Rice, J. E.; Schaefer, H. F. *J. Chem. Phys.* **1987**, *86*, 2881.

(60) Piecuch, P.; Paldus, J. *Int. J. Quantum Chem.* **1989**, *36*, 429.

(61) Raghavachari, K.; Trucks, G. W.; Pople, J. A.; Head-Gordon, M. *Chem. Phys. Lett.* **1989**, *157*, 479.

(62) Kowalski, K.; Piecuch, P. *J. Chem. Phys.* **2000**, *113*, 5644.

(63) Kowalski, K.; Piecuch, P. *J. Chem. Phys.* **2000**, *113*, 18.

(64) Piecuch, P.; Kowalski, K. In *Computational Chemistry: Reviews of Current Trends*; Leszczyński, J., Ed.; World Scientific: Singapore, 2000; Vol. 5, p 1.

(65) Piecuch, P.; Kowalski, K.; Pimienta, I. S. O.; McGuire, M. J. *Int. Rev. Phys. Chem.* **2002**, *21*, 527.

(66) Piecuch, P.; Pimienta, I. S. O.; Fan, P.-D.; Kowalski, K. In *Progress in Theoretical Chemistry and Physics*; Maruani, J., Lefebvre, R., Brändas, E., Eds.; Kluwer: Dordrecht, The Netherlands, 2003; Vol. 12, p 119.

(67) Piecuch, P.; Kowalski, K.; Pimienta, I. S. O.; Fan, P.-D.; Lodriguito, M.; McGuire, M. J.; Kucharski, S. A.; Kuœ, T.; Musiał, M. *Theor. Chem. Acc.* **2004**, *112*, 349.

(68) Kowalski, K.; Piecuch, P. *Chem. Phys. Lett.* **2001**, *344*, 165.

(69) Piecuch, P.; Kucharski, S. A.;

(70) McGuire, M. J.; Kowalski, K.; Piecuch, P. *J. Chem. Phys.* **2002**, *117*, 3617.

(71) McGuire, M. J.; Piecuch, P.; Kowalski, K.; Kucharski, S. A.; Musiaš, M. *J. Phys. Chem. A* **2004**, *108*, 8878.

(72) Kowalski, K.; Piecuch, P. *J. Chem. Phys.* **2005**, *122*, 074107.

(73) Piecuch, P.; Kowalski, K.; Pimienta, I. S. O.; Kucharski, S. A. In *Low-Lying Potential Energy Surfaces*; Hoffmann, M. R., Dyall, K. G., Eds.; American Chemical Society: Washington, DC, 2002; Vol. 828, p 31.

(74) Özkan, I.; Kinal, A.; Balci, M. *J. Phys. Chem. A* **2004**, *108*, 507.

(75) McGuire, M. J.; Piecuch, P. *J. Am. Chem. Soc.* **2005**, *127*, 2608.

(76) Kinal, A.; Piecuch, P. *J. Phys. Chem. A* **2006**, *110*, 367.

(77) Włoch, M.; Lodriguito, M. D.; Piecuch, P.; Gour, J. R. *Mol. Phys.* **2006**, *104*, 2149.

(78) Piecuch, P.; Włoch, M. *J. Chem. Phys.* **2005**, *123*, 224105.

(79) Piecuch, P.; Włoch, M.; Gour, J. R.; Kinal, A. *Chem. Phys. Lett.* **2005**, *418*, 463.

(80) Hirata, S.; Fan, P.-D.; Auer, A. A.; Nooijen, M.; Piecuch, P. *J. Chem. Phys.* **2004**, *121*, 12197.

(81) Piecuch, P.; Włoch, M.; Varandas, A. J. C. In *Progress in Theoretical Chemistry and Physics*; Lahmar, S., Maruani, J., Wilson, S., Delgado-Barrio, G., Eds.; Springer: Berlin, 2007; Vol. 16.

(82) Roos, B. O. In *Ab Initio Methods in Quantum Chemistry*; Lawley, K. P., Ed.; Wiley: New York, 1987; Vol. 2, p 399.

(83) Andersson, K.; Malmqvist, P.-Å.; Roos, B. O.; Sadlej, A. J.; Wolinski, K. *J. Phys. Chem.* **1990**, *94*, 5483.

(84) Finley, J.; Malmqvist, P.-Å.; Roos, B. O.; Serrano-Andres, L. *Chem. Phys. Lett.* **1998**, *288*, 299.

(85) Roos, B. O.; Andersson, K.; Fülscher, M. P.; Serrano-Andrés, L.; Pierloot, K.; Merchán, M.; Molina, V. *J. Mol. Struct. (THEOCHEM)* **1996**, *388*, 257.

(86) Ghigo, G.; Roos, B. O.; Malmqvist, P.-Å. *Chem. Phys. Lett.* **2004**, *396*, 142.

(87) Douglas, M.; Kroll, N. M. *Ann. Phys.* **1974**, *82*, 89.

(88) Hess, B. A. *Phys. Rev. A* **1986**, *33*, 3742.

(89) Persson, B. J.; Roos, B. O.; Pierloot, K. *J. Chem. Phys.* **1994**, *101*, 6810.

(90) Gagliardi, L.; Roos, B. O. *Inorg. Chem.* **2003**, *42*, 1599.

(91) Ghosh, A.; Taylor, P. R. *Curr. Opin. Chem. Biol.* **2003**, *7*, 113.

(92) Flock, M.; Pierloot, K. *J. Phys. Chem. A* **1999**, *103*, 95.

(93) Siegbahn, P. E. M. *Q. Rev. Biophys.* **2003**, *36*, 91.

(94) Lind, T.; Siegbahn, P. E. M.; Crabtree, R. H. *J. Phys. Chem. B* **1999**, *103*, 1193.

(95) Siegbahn, P. E. M. *J. Biol. Inorg. Chem.* **2003**, *8*, 577.

(96) Siegbahn, P. E. M. *J. Biol. Inorg. Chem.* **2003**, *8*, 567.

(97) Siegbahn, P. E. M.; Wirstam, M. *J. Am. Chem. Soc.* **2001**, *123*, 11819.

(98) Mirica, L. M.; Vance, M.; Rudd, D. J.; Hedman, B.; Hodgson, K. O.; Solomon, E. I.; Stack, T. D. P. *Science* **2005**, *308*, 1890.

(99) Kowalski, K.; Piecuch, P. *J. Chem. Phys.* **2004**, *120*, 1715.

(100) Metz, M.; Solomon, E. I. *J. Am. Chem. Soc.* **2001**, *123*, 4938.